11

Recursive Subtraction of UV-Divergences by R-Operation

The recursive counterterm procedure developed by Bogoliubov, Parasiuk, and Hepp [1], which was briefly described at the beginning of Chapter 9, yields a finite result for each Feynman diagram, order by order in perturbation theory. It is useful to interprete this procedure as an application of a *R-operation* to the Feynman diagram. All the finite results on higher loops in this book will be derived via the R-operation.

We shall not follow a possible alternative approach based on a general solution of the recursion relation developed by Zimmermann [2], who specified the R-operation by a complete diagrammatic expansion in the form of a so-called *forest formula*. With this formula, the renormalization procedure is known as the *BPHZ formalism*. It was applied by Zimmermann directly to the integrands of the Feynman integrals, making them manifestly convergent without regularization. Subsequently, several authors showed that the R-operation leads to the same finite results, if applied individually to the Feynman integrals regularized by minimal subtraction [3].

The chapter will end with a discussion of the general structure of the counterterms. This will show how the minimal subtraction scheme considerably reduces the number of relevant diagrams to be evaluated explicitly.

In the following manipulations, the negative coupling constant $-\lambda$ associated with each vertex will be omitted, unless otherwise stated, since they will be of no relevance to the analytic expressions represented by the Feynman diagrams.

11.1 Graph-Theoretic Notations

For recursive diagrammatic subtractions of divergences, some graph-theoretic concepts are useful. The first important concept of a *subdiagram* was introduced before, after Eq. (9.3). It will also be useful to admit to the set of all subdiagrams the original diagram itself. If this is excluded, we speak otherwise of a *proper subdiagram*. The notation will be $\gamma \subset G$ for subdiagrams and $\bar{\gamma} \subset G$ for proper subdiagrams of the diagram G. Then we define

- a *shrunk diagram* G/γ, obtained from G by shrinking all lines in γ to zero length, so that their endpoints coincide. Each connected part of γ then collapses to a single vertex.

As an example, consider the five-loop diagram

$G =$ 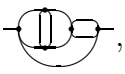 ,

with the two-loop subdiagram

$\gamma =$  .

By shrinking all lines of the subdiagram, we find the shrunk diagram

$G/\gamma =$  .

Next we define

- UV-divergent 1PI subdiagrams γ_i of G to be *UV-disjoint in* G if they have no internal line (I) and no vertex (V) in common.

Note that a UV-divergent 1PI diagram cannot consist of UV-disjoint components only. Even if the components of a diagram are merely connected by a cutvertex (to be defined in the next item below), the components cannot be UV-disjoint subdiagrams in G because they have a vertex in common. A set of UV-disjoint subdiagrams $\gamma \subset G$ will be denoted by $\Gamma(G)$:

$$\Gamma = \{\gamma | \gamma \in G, \gamma \text{ UV-disjoint}\}. \tag{11.1}$$

For proper UV-disjoint subdiagrams $\bar{\gamma}$, the notation will be $\bar{\Gamma}(G)$. The detailed set-theoretic definition for $\bar{\Gamma}(G)$ is

$$\bar{\Gamma}(G) = \{\bar{\gamma}_i | \bar{\gamma}_i \subset G,\ 1\text{PI},\ \omega(\bar{\gamma}_i) \geq 0,\ I(\bar{\gamma}_i \cap \bar{\gamma}_j) = 0,\ V(\bar{\gamma}_i \cap \bar{\gamma}_j) = 0\}\,.$$

We furthermore introduce the set of all sets $\Gamma(G)$ or $\bar{\Gamma}(G)$ contained in a diagram G, denoting them by Γ_G or $\bar{\Gamma}_G$:

$$\bar{\Gamma}_G = \{\text{all } \bar{\Gamma}(G)\} \quad \text{and} \quad \Gamma_G = \{\text{all } \Gamma(G)\} \quad \text{with} \quad \Gamma_G = \bar{\Gamma}_G \cup \{G\}\,. \tag{11.2}$$

Two sets $\Gamma(G)$ of UV-disjoint subdiagrams of G can never contain the same integrations.

Finally, we introduce the concept of a cutvertex:

- A diagram G is said to contain a *cutvertex* if it can be decomposed into two components G_1 and G_2 by cutting it at a vertex. Each of the components is defined to include the vertex where the cut is made. The same definition holds for subdiagrams γ decomposing into components γ_1 and γ_2.

As an example, the complete set $\bar{\Gamma}_G$ of all sets $\bar{\Gamma}(G)$ of proper UV-disjoint subdiagrams $\bar{\gamma} \in G$ for the diagram

$G =$ 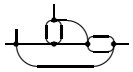

is

$\bar{\Gamma}_G = \{\,\bar{\Gamma}(G)\,\} =$ 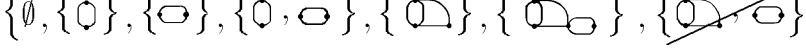

The last set $\bar{\Gamma}(G)$ is forbidden since it contains subdiagrams which have a common vertex. In fact, this last set and the one before contain the same integrations, which would have led to double-counting. Another example will be discussed below in Eqs. (11.16)–(11.19).

11.2 Definition of R- and $\bar{R}$-Operation

The R-operation is defined as follows: when applied to a diagram G, it subtracts shrunk diagrams in such a way that RG is free of divergences. In dimensional regularization, all divergences are of the form $1/\varepsilon^i$, such that RG contains, by definition, no such terms, and is finite for $\varepsilon \to 0$. In terms of the $\mathcal{K}$-operation defined in Eq. (9.76), which selects precisely all $1/\varepsilon^i$ terms of a Feynman integral, we may state this property as

$$\mathcal{K}RG = 0 \quad \text{for any} \quad \omega(G). \tag{11.3}$$

Application of the R-operation to G removes all divergences coming from subdiagrams, and the superficial divergence of G itself. In the above set-theoretic notation, the result of the R-operation may be stated as follows: the first term in RG is G itself. From this, all possible diagrams are subtracted in which the integration over some divergent subdiagrams is substituted by the corresponding counterterm. Among these, there is the term in which the whole integration of G is substituted by the corresponding counterterm. This is the term we are looking for. The remainder consists of a sum over all sets $\bar{\Gamma}(G)$, which contain all possible arrangements of divergent subdiagrams without double-counting. Let us denote by Δ_γ the counterterm associated with a subdiagram γ, i.e., the pole term of the superficial divergence of this subdiagram. This differs, in general, from $\mathcal{K}(\gamma)$ by possible pole terms of subdivergences. With this notation, the result of the R-operation may be written as

$$\begin{aligned} RG &= G + \sum_{\Gamma\neq\emptyset} \prod_{\gamma_i\in\Gamma} \Delta_{\gamma_i} * G/\Gamma \\ &= \sum_{\Gamma} \prod_{\gamma_i\in\Gamma} \Delta_{\gamma_i} * G/\Gamma, \end{aligned} \tag{11.4}$$

with $\Delta_\emptyset * G/\emptyset = G$. The sum over Γ runs over all UV-disjoint subdiagrams $\Gamma(G) \in \Gamma_G$. The shrunk integral G/Γ stands for the integral of G without propagators and integrations of the subdiagrams contained in $\Gamma(G)$. Diagrammatically, each subdiagram contained in Γ is shrunk to a vertex in G. Remember that the vertices no longer represent the negative coupling constant. Recall also that, by definition in Eq. (9.122), the operation $*$ implies the substitution of the counterterm into the remaining integrations of the shrunk diagram. For a UV-divergent subdiagram γ, the integrand of G can be written as $I_G(\mathbf{k}) = I_\gamma(\mathbf{p},\mathbf{q})\, I_{G/\gamma}(\mathbf{q},\mathbf{l},\mathbf{k})$, where $\mathbf{k}$ and $\mathbf{q}$ are the external momenta of G and γ, respectively, whereas $\mathbf{p}$ stands for the momenta of integration in γ. The momenta $\mathbf{q}$, $\mathbf{l}$ appear in the loop integrals of G/γ. The subtracted terms are then constructed from the original Feynman diagram of G as follows:

$$G = \int \frac{d^Dq}{(2\pi)^D}\,\gamma(\mathbf{q}) I_{G/\gamma}(\mathbf{q},\mathbf{l},\mathbf{k}) \;\longrightarrow\; \Delta_\gamma * G/\gamma = \int \frac{d^Dq}{(2\pi)^D} \int \frac{d^Dl}{(2\pi)^D}\,\Delta_\gamma(\mathbf{q})\, I_{G/\gamma}(\mathbf{q},\mathbf{l},\mathbf{k}).$$

In Section 9.3.2, this construction was carried out explicitly for the renormalization up to two loops.

For a logarithmically divergent subdiagram γ, the counterterm is independent of the external momenta of γ, consisting only of $1/\varepsilon^i$-poles: $\Delta_\gamma = \mathcal{Z}_\gamma(\varepsilon^{-1})$. For this reason, the counterterms of the subdiagram γ do not contribute to the integrals in the full diagram, and the operation $*$ reduces to a simple multiplication:

$$\Delta_\gamma * G/\gamma = \mathcal{Z}_\gamma(\varepsilon^{-1}) \int \frac{d^Dq}{(2\pi)^D} \int \frac{d^Dl}{(2\pi)^D}\, I_{G/\gamma}(\mathbf{q},\mathbf{l},\mathbf{k}). \tag{11.5}$$

In this case, we usually omit the symbol $*$, unless required for clarity.

The operation $*$ becomes nontrivial for quadratically divergent subdiagrams γ, as we have seen already in Eq. (9.100), and as will be discussed in detail in Section 11.6. Then the counterterms for the two-point vertex function contain contributions proportional to m^2 and to $\mathbf{p}^2$, where $\mathbf{p}$ is the external momentum of the subdiagram. In this case, $\mathbf{p}^2$ will participate in the integration of the total diagram. Writing the associated counterterm in the generic form $\Delta_\gamma = \mathbf{q}^2\,\mathcal{Z}'_\gamma(\varepsilon^{-1})$, the counterterm diagram contributes the Feynman integral

$$\Delta_\gamma * G/\gamma = \mathcal{Z}'_\gamma(\varepsilon^{-1}) \int \frac{d^Dq}{(2\pi)^D} \int \frac{d^Dl}{(2\pi)^D}\, \mathbf{q}^2 I_{G/\gamma}(\mathbf{q},\mathbf{l},\mathbf{k})\,. \tag{11.6}$$

Actually, the relevant calculations will eventually be carried out at zero mass, such that (11.6) will be the only integral to be evaluated. An example for this procedure will be treated in Eq. (12.18).

Let us abbreviate the product of the counterterms of the subdiagrams contained in Γ by the symbol Δ_Γ:

$$\Delta_\Gamma = \prod_{\gamma_i \in \Gamma} \Delta_{\gamma_i}, \tag{11.7}$$

the R-operation in Eq. (11.4) may be written as

$$RG = \sum_\Gamma \Delta_\Gamma * G/\Gamma. \tag{11.8}$$

Then we separate the term $\Gamma = \{G\}$ from the sum, and apply the operator $\mathcal{K}$ as follows:

$$\mathcal{K}\,\Delta_G G/G + \mathcal{K} \sum_{\bar\Gamma} \Delta_{\bar\Gamma} * G/\bar\Gamma = 0\,. \tag{11.9}$$

The sum runs now over all $\bar\Gamma(G) \neq \{G\}$. In minimal subtraction, $\mathcal{K}\Delta_G = \Delta_G$, and $G/G = 1$, so that we find the counterterm Δ_G of G as

$$\Delta_G = -\mathcal{K} \sum_{\bar\Gamma} \Delta_{\bar\Gamma} * G/\bar\Gamma. \tag{11.10}$$

It is useful to define the negative of the right-hand side as the result of a so-called *incomplete R-operation*, or *$\bar R$-operation*,

$$\mathcal{K}\bar R G \equiv \mathcal{K} \sum_{\bar\Gamma} \Delta_{\bar\Gamma} * G/\bar\Gamma = \mathcal{K} \sum_{\bar\Gamma} \prod_{\gamma_i \in \bar\Gamma} \Delta_{\gamma_i} * G/\bar\Gamma\,. \tag{11.11}$$

With the help of Eq. (11.10), we now express the counterterm Δ_γ of any subdiagram γ as the result of an $\bar R$-operation applied to γ:

$$\Delta_\gamma = -\mathcal{K}\bar R \gamma\,. \tag{11.12}$$

Inserting this into (11.11), we find the counterterm Δ_G as a result of a recursive application of the $\bar R$-operation:

$$\begin{aligned} \Delta_G = -\mathcal{K}\bar R G \;&=\; -\mathcal{K} \sum_{\bar\Gamma} \prod_{\gamma \in \bar\Gamma} (-\mathcal{K}\bar R \gamma) * G/\bar\Gamma \\ &=\; -\mathcal{K}\Big[G + \sum_{\bar\Gamma \neq \emptyset} \prod_{\gamma \in \bar\Gamma} (-\mathcal{K}\bar R \gamma) * G/\bar\Gamma\Big]. \end{aligned} \tag{11.13}$$

This formula is used to calculate all counterterms up to five loops, as shown explicitly in Appendix A.

As an illustration of the recursive procedure, let us recalculate the second-order counterterms to $\bar\Gamma^{(2)}(\mathbf{k})$ in Section 9.3.2 in terms of the $\bar R$-operation. Since the vertices do not contain the coupling constants as in the previous chapters, we must write them down explicitly as prefactors of each diagram. Remembering the diagrammatic expansion in the first equation of (9.12), we have the equation for the pole terms

$$\mathcal{K}\bar R\bar\Gamma^{(2)} = \Big[-g\mu^\varepsilon \frac{1}{2}\mathcal{K}\bar R(\;\underset{\sim}{\bigcirc}\;) + g^2\mu^{2\varepsilon}\frac{1}{4}\mathcal{K}\bar R(\;\underset{\sim}{\bigcirc\!\!\times\!\!\bigcirc}\;) + g^2\mu^{2\varepsilon}\frac{1}{6}\mathcal{K}\bar R(\;\multimap\!\!\bigcirc\!\!\multimap\;)\Big]\,. \tag{11.14}$$

Performing the $\bar{R}$-operation on the two-loop diagrams yields

$$\begin{aligned}
\mathcal{K}\bar{R}(\ \underline{\bigcirc}\ ) &= \mathcal{K}\,\underline{\bigcirc}\ , \\
\mathcal{K}\bar{R}(\ \underline{\bigcirc\!\!\bigcirc}\ ) &= \mathcal{K}\Big(\underline{\bigcirc\!\!\bigcirc} - \mathcal{K}(\ \underline{\bigcirc}\ ) * \underline{\bigcirc} - \mathcal{K}(\ \underline{\bigcirc}\ ) * \underline{\bigcirc}\ \Big), \\
\mathcal{K}\bar{R}(\ \underline{\ominus}\ ) &= \mathcal{K}\Big(\underline{\ominus} - 3\mathcal{K}(\ \underline{\times}\ ) * \underline{\bigcirc}\ \Big).
\end{aligned}$$

Note the factor three in the subtraction in the last line. The subdiagram is indeed contained three times in the diagram. This is an example of the treatment of overlapping divergence by the subtraction method. Together with Eqs. (9.121) and (9.122), the right-hand side of Eq. (11.14) can be rewritten in terms of counterterm diagrams:

$$\mathcal{K}\bar{R}\bar{\Gamma}^{(2)} = \mathcal{K}\Big[- g\mu^{\varepsilon}\frac{1}{2}\,\underline{\bigcirc}\ + g^2\mu^{2\varepsilon}\frac{1}{4}\,\underline{\bigcirc\!\!\bigcirc}\ + g^2\mu^{2\varepsilon}\frac{1}{2}\,\underline{\bigcirc}\!\!\bigcirc\ + g^2\mu^{2\varepsilon}\frac{1}{2}\,\underline{\bigcirc\!\!\bullet}\ + g^2\mu^{2\varepsilon}\frac{1}{6}\,\underline{\ominus}\ \Big]. \quad (11.15)$$

Apart from the explicit prefactors $-g\mu^{\varepsilon}$, this is precisely the previous expression (9.94) for the pole terms.

11.3 Properties of Diagrams with Cutvertices

A cutvertex has the generic diagrammatic form

$$G = \quad = G_1 \cdot G_2. \quad (11.16)$$

The integrations in each component G_1 and G_2 are obviously independent, and so are the associated divergences. Hence the counterterm of G must be the product of the counterterms of the two components:

$$\Delta_G = -\mathcal{K}\bar{R}G = (\ -\mathcal{K}\bar{R}G_1) \cdot (\ -\mathcal{K}\bar{R}G_2) = \Delta_{G_1} \cdot \Delta_{G_2}. \quad (11.17)$$

Since each nonzero Δ_G contains at least a simple pole in ε, the counterterm of a cutvertex contains a pole ε^{-n} with $n \geq 2$. In Eqs. (10.43)–(10.46), we have learned that the renormalization group functions in the MS-scheme consist only of the simple poles of the counterterms. As a consequence, diagrams with cutvertices do not contribute to the renormalization group functions.

The simplest example for relation (11.17) is the diagram $G =$. Applying $\mathcal{K}\bar{R}$ to this yields

$$\mathcal{K}\bar{R}(\ \ ) = \mathcal{K}\Big[\ \ - 2\,\mathcal{K}(\ \ )\ \ \Big]\ . \quad (11.18)$$

The first term on the right-hand side can be rewritten as

$$\mathcal{K}(\ \ ) \ = \ \mathcal{K}\Big[- \mathcal{K}(\ \ )\mathcal{K}(\ \ ) + 2\,\mathcal{K}(\ \ )\ \ \Big], \quad (11.19)$$

implying that the pole terms factorize:

$$\mathcal{K}\bar{R}(\ \ ) = -\mathcal{K}(\ \ )\mathcal{K}(\ \ ).$$

Let us also give an example for the effect of the $\bar{R}$-operation upon a more complicated three-loop diagram, in which these pole terms appear in a subdiagram:

$$\mathcal{K}\bar{R}(\ \ ) \ = \ \mathcal{K}\Big[\ \ - \mathcal{K}(\ \ )\ \ - \mathcal{K}(\ \ )\ \ - \mathcal{K}\bar{R}(\ \ )\ \ \Big]\ . \quad (11.20)$$

The last subtraction term contains the cutvertex, whose pole terms factorize as

$$\mathcal{K}\bar{R}(\;\text{  }\;) = -\mathcal{K}(\;\text{  }\;)\mathcal{K}(\;\text{}\;)\;. \tag{11.21}$$

The right-hand side does not appear in (11.20) since the two subdiagrams are not UV-disjoint in G. Remember that the sets $\bar{\Gamma}(G)$ were defined to contain only UV-disjoint subdiagrams, in order to avoid a double subtraction of $(-\mathcal{K}\bar{R}G_1)\cdot(-\mathcal{K}\bar{R}G_2)$ and of $-\mathcal{K}\bar{R}G$.

As a consequence of (11.16), all four-point chain diagrams like

$$\text{  }\;, \quad \text{}\;, \quad \text{}\;, \tag{11.22}$$

do not contribute to the RG-functions. Their counterterms are, by formula $\left[-\mathcal{K}(\;\text{  }\;)\right]^n \propto 1/\varepsilon^n$, free of simple poles in ε. But only these simple poles survive in the calculation of β, γ, and γ_m, as we have seen in Section 10.3. In the five-loop calculation in Chapter 15, we shall nevertheless list the full renormalization constants including all higher poles. The cancellation of these poles in the calculation of the renormalization group functions provides us with a useful check of the lower ones.

For the contribution of the chain diagrams to the mass counterterm in the two-point function see the discussion after Eq. (11.42).

11.4 Tadpoles in Diagrams with Superficial Logarithmic Divergence

Diagrams or subdiagrams of the form pictured in Fig. 11.1 are called *tadpole diagrams*, *tadpole parts* of a diagram, or briefly *tadpoles*. The name tadpole referred originally to diagrams which have the shape of a biological tadpole drawn on the left-hand side in Fig. 11.1. Such diagrams occur in ϕ^3-theories or in perturbation expansions of ϕ^4-theories in the ordered phase, which is not considered here. In the disordered phase under study, analogous diagrams occur with two legs, as shown on the right-hand side of the figure. Similar diagrams occur, incidentally, in quantum electrodynamics, where they are more appropriately called "seagull" diagrams, since they look more like (somewhat fat) seagulls on the ocean sky. More generally, we shall define as tadpole diagrams all diagrams which are quadratically divergent and contain no external momenta. Tadpole diagrams have therefore only one external vertex, which is a cutvertex if the tadpole is a subdiagram. Thus tadpole diagrams renormalize only the mass. In the present theory, the simplest tadpole diagram is  .

Diagrams with a tadpole part produce counterterms only if they are quadratically divergent by power counting. If they are merely logarithmically divergent, thus possessing an equal number of momenta in numerator and denominator of the integrand, the subdiagram to which the tadpole part is attached has two momentum powers less in the numerator and therefore no superficial divergence by power counting. Thus, if we apply the $\bar{R}$-operation to such a

FIGURE 11.1 Structure of tadpole diagrams. The left figure sketches the shape of a biological tadpole. The right figure shows the shape of the "tadpole diagrams" occurring in the normal phase of ϕ^4-theories, which really look like seagulls. Logarithmically divergent Feynman diagrams containing these as subdiagrams do not contribute in dimensional regularization.

diagram and use the factorization property of diagrams with cutvertices as discussed in the last subsection, we obtain zero. An example is:

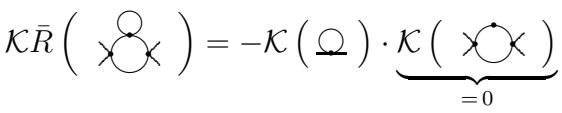

(11.23)

For quadratically divergent diagrams, the factorized subdiagram is still logarithmically divergent, such that the operation $\mathcal{K}\bar{R}$ does yield a nonzero counterterm.

11.5 Nontrivial Example for $\bar{R}$-Operation

A good nontrivial example for the application of the $\bar{R}$-operation is the five-loop diagram

which appears in the complete list of recursive diagrammatic expansions in Appendix A on page 424 as No. 59. It contains a subdiagram with a cutvertex. The first step in the recursion yields

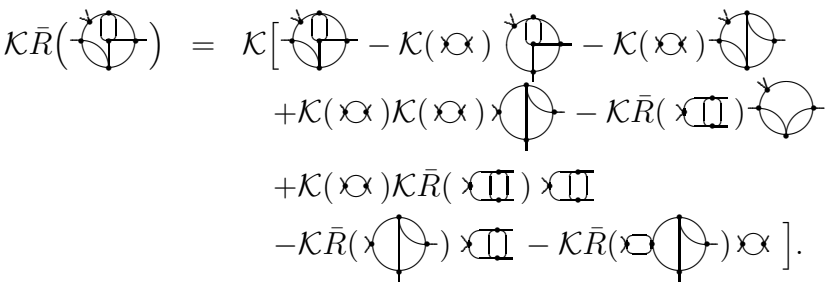

(11.24)

A second step is necessary in the fifth and sixth term:

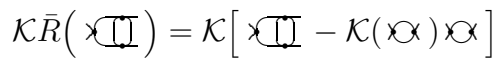

(11.25)

The last term in (11.24) factorizes at its cutvertex

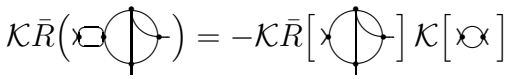

(11.26)

and only the first component, which also appears in the second-last term in (11.24), requires further consideration. It is expanded as

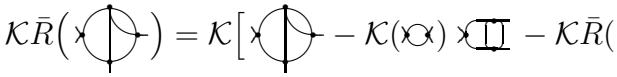

(11.27)

The right-hand side contains only pole terms of lower-order and shrunk diagrams.

11.6 Counterterms in Minimal Subtraction

Renormalizability requires the counterterms to have the general local form described in Section 9.3. As explained in Subsection 9.3.1, the counterterms are further simplified by using

minimal subtraction. For the proofs of the renormalizability in the context of dimensional regularization see Ref. [3].

The first step in such proofs consists in showing that application of the R-operation to a diagram G yields a Feynman integral RG which is indeed free of subdivergences, and that the counterterms subtracted to achieve this are all local. The proof proceeds by induction in the number of loops.

As already mentioned in Subsection 9.3.3 and 11.2, we have to make sure that the combinatorics of the subtractions in each diagram allow for a complete absorption of all $1/\varepsilon^i$ -terms via counterterms by a redefinition of the parameters in the energy functional. This is not obvious since the counterterm diagrams subtract the subdivergences of different diagrams. Some work is necessary to demonstrate that the combinatorics of the subtraction scheme reproduces the correct weight factors of the counterterms. At the end one verifies that the counterterms can indeed be found as the sum of the pole terms $\mathcal{K}\bar{R}G$ of the individual diagrams G. They are polynomials in the external momenta with a maximal power $\mathbf{k}^2$ allowed by locality. In ϕ^4-theory, all divergences appear in the two- and four-point functions. The pole terms $\mathcal{K}\bar{R}\bar{\Gamma}^{(2)}$ contain only terms proportional to m^2 and $\mathbf{k}^2$, whereas $\mathcal{K}\bar{R}\bar{\Gamma}^{(4)}$ contains no momenta at all:

$$-\mathcal{K}\bar{R}\bar{\Gamma}^{(2)}(\mathbf{k}) = \mathcal{K}\bar{R}(\Sigma) \quad \longrightarrow \quad m^2 c_{m^2}(g,\varepsilon^{-1}) + \mathbf{k}^2 c_\phi(g,\varepsilon^{-1})\,, \tag{11.28}$$

$$-\mathcal{K}\bar{R}\bar{\Gamma}^{(4)}(\mathbf{k}_i) \quad \longrightarrow \quad \mu^\varepsilon g\, c_g(g,\varepsilon^{-1})\,. \tag{11.29}$$

This is the general form of the counterterms leading to a local counterterm energy functional (9.63) [recall Eqs. (9.65)–(9.67)].

The counterterms are expansions in g and ε^{-1} independent of the mass and the external momentum and have the generic form (9.1). No additional divergences appear for the critical theory with $m^2 = 0$. The trivial mass- and $\mathbf{k}^2$-dependences permit us to rewrite the renormalization constants as follows:

$$Z_{m^2}(g,\varepsilon^{-1}) = 1 - \mathcal{K}\bar{R}\frac{\partial}{\partial m^2}\,\bar{\Gamma}^{(2)}(\mathbf{k})\,, \tag{11.30}$$

$$Z_\phi(g,\varepsilon^{-1}) = 1 - \mathcal{K}\bar{R}\frac{\partial}{\partial \mathbf{k}^2}\,\bar{\Gamma}^{(2)}(\mathbf{k})\,, \tag{11.31}$$

$$Z_g(g,\varepsilon^{-1}) = 1 - \mathcal{K}\bar{R}\frac{1}{\mu^\varepsilon g}\,\bar{\Gamma}^{(4)}(\mathbf{k}_i)\,. \tag{11.32}$$

In writing them down , we have made use of the fact that the operations $\mathcal{K}$ and $\bar{R}$ commute with the differentiations with respect to m^2 and $\mathbf{k}^2$. This follows from the absolute convergence of the initial Feynman integrals in $D = 4 - \varepsilon$ dimensions with $\varepsilon \neq 0$. Performing the differentiations under the integrals, their superficial degree of divergence is lowered by two, and all integrals on the right-hand side of Eqs. (11.30)–(11.32) become logarithmically divergent.

The calculation of all three renormalization constants simplifies in minimal subtraction because diagrams with tadpole subdiagrams do not contribute. For Z_g this is due to the fact that all divergences contributing to the vertex function $\bar{\Gamma}^{(4)}(\mathbf{k}_i)$ are at most logarithmically divergent, and we have shown in Section 11.4 that a tadpole subdiagram causes the remaining diagram to be superficially convergent. Thus the total Feynman integral vanishes under the application of $\mathcal{K}\bar{R}$.

For the renormalization constants Z_{m^2} and Z_ϕ, additional simplifications arise, which we shall now discuss.

11.7 Simplifications for Z_{m^2}

Differentiating a propagator with respect to m^2 raises the power of momenta in the denominator by two. The resulting Feynman integral may be viewed diagrammatically as having arisen from the insertion of an extra $-\phi^2$-vertex with two legs (recall Sections 2.4 and 3.5):

$$\frac{\partial}{\partial m^2}\,\frac{1}{\mathbf{p}^2+m^2} = \frac{-1}{(\mathbf{p}^2+m^2)^2} \;\hat{=}\; \frac{\partial}{\partial m^2}\;\text{—}\;=\;\text{—•} \;. \tag{11.33}$$

The two additional powers of momenta in the denominator lower the superficial degree of divergence ω by two, changing a quadratic divergence into a logarithmic one. With the product rule of differentiation, application of $\partial/\partial m^2$ to diagrams with several lines leads to a sum of logarithmically divergent diagrams, each containing an extra $-\phi^2$-vertex. If n lines are indistinguishable, the differentiation results in a multiplicity factor n, which is 3 in the following example:

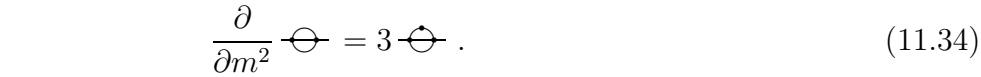

$$\frac{\partial}{\partial m^2}\;\text{⊖}\;=3\;\text{⊖•}\;. \tag{11.34}$$

The logarithmically divergent Feynman integral of the diagram on the right-hand side corresponds to a diagram ⊖ of the four-point vertex function of $\bar{\Gamma}^{(4)}(\mathbf{k}_i)$, in which the external momenta incoming at the above ϕ^2-vertex have been set equal to zero. For dimensional reasons, the external momenta do not appear in the counterterms $\mathcal{K}\bar{R}G$ of a logarithmically divergent integral G, and the differentiated Feynman integral used for the mass renormalization produces the same counterterm as the corresponding integral in $\bar{\Gamma}^{(4)}(\mathbf{k}_i)$. In the $\mathcal{K}\bar{R}$-notation, we may write:

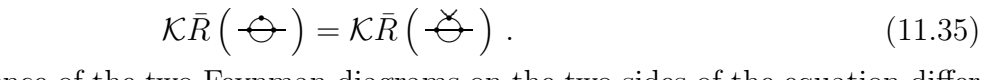

$$\mathcal{K}\bar{R}\left(\text{⊖•}\right)=\mathcal{K}\bar{R}\left(\text{⊖}\right)\;. \tag{11.35}$$

The superficial divergence of the two Feynman diagrams on the two sides of the equation differ only in the power of the coupling constant associated with the vertex on the top. Having set g equal to unity, we see that the two sides are identical.

Another example illustrates the differentiation of quadratically divergent diagrams with a tadpole part:

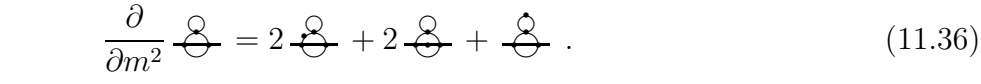

$$\frac{\partial}{\partial m^2}\;\text{◎⊖}\;=2\;\text{◎⊖•}\;+2\;\text{◎•⊖}\;+\;\text{•◎⊖}\;. \tag{11.36}$$

The R-operation applied to the two logarithmically divergent diagrams in Eq. (11.36), which contain a tadpole part, gives zero as explained in Section 11.4:

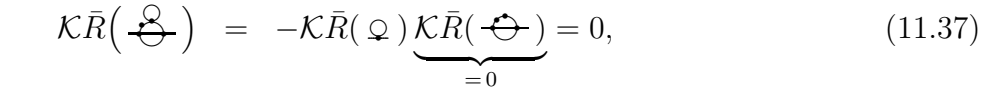

$$\mathcal{K}\bar{R}\Big(\text{◎⊖•}\Big) \;=\; -\mathcal{K}\bar{R}(\,\text{◎}\,)\underbrace{\mathcal{K}\bar{R}(\,\text{⊖•}\,)}_{=0}=0, \tag{11.37}$$

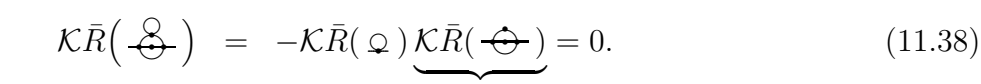

$$\mathcal{K}\bar{R}\Big(\text{◎⊖•}\Big) \;=\; -\mathcal{K}\bar{R}(\,\text{◎}\,)\underbrace{\mathcal{K}\bar{R}(\,\text{⊖•}\,)}_{=0}=0. \tag{11.38}$$

The pole terms in the third diagram of Eq. (11.36), which has a $-\phi^2$-vertex inserted into the tadpole part, is a product of the pole terms of two logarithmically divergent diagrams:

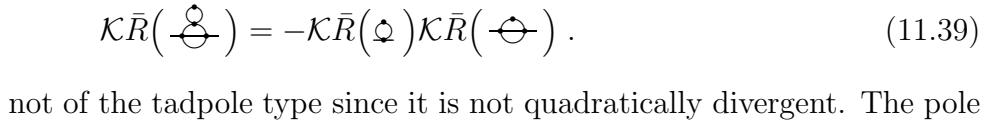

$$\mathcal{K}\bar{R}\Big(\text{•◎⊖}\Big)=-\mathcal{K}\bar{R}\Big(\text{•◎}\Big)\mathcal{K}\bar{R}\Big(\text{⊖•}\Big)\;. \tag{11.39}$$

The subdiagram •◎ is not of the tadpole type since it is not quadratically divergent. The pole terms of this diagram were considered earlier in Eq. (9.79), where we showed that

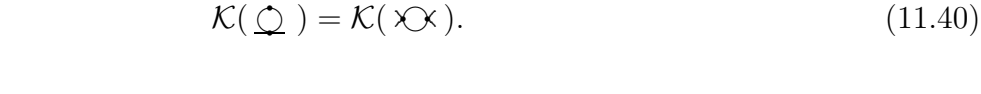

$$\mathcal{K}(\,\text{•◎}\,)=\mathcal{K}(\,\text{×◎×}\,). \tag{11.40}$$

Hence the counterterm contribution of the whole diagram on the left-hand side of Eq. (11.36) is the same as that of a four-point diagram renormalizing the coupling constant:

$$\frac{\partial}{\partial m^2}\,\mathcal{K}\bar{R}$$ $$= \mathcal{K}\bar{R}\Big($$  $$\Big) = \mathcal{K}\bar{R}\Big($$  $$\Big)\,. \tag{11.41}$$

Another example are all two-point chain diagrams consisting of simple bubbles like the following:

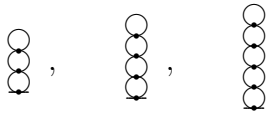 . (11.42)

After the differentiation with respect to the mass, we are left with the contributions of the following four-point diagrams:

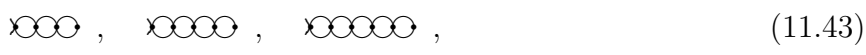 , (11.43)

whereas all diagrams with ϕ^2-insertions in any other line give zero upon application of the $\bar{R}$-operation. The remaining diagrams have the same counterterm contribution as the four-point chain diagrams (11.22) and, like those, they contribute to the renormalization constants only with higher poles which cancel when calculating the renormalization group functions.

These examples suggest that the diagrams contributing to the mass renormalization form a subset of the diagrams contributing to the coupling constant renormalization. This can be observed to all orders in perturbation theory. The subset consists of all four-point diagrams without tadpole parts, and with two external lines entering at one common vertex. After dropping a factor $-\mu^\varepsilon g$, and multiplying everything with the appropriate weight factors and symmetry factors, we obtain directly the contribution to the mass renormalization factor $Z_{m^2}(g,\varepsilon^{-1})$.

11.8 Simplifications for Z_ϕ

The calculation of $Z_\phi(g,\varepsilon^{-1})$ is also simplified by the fact that all diagrams with tadpole subdiagrams do not contribute. Here this happens for a different reason than in $Z_{m^2}(g,\varepsilon^{-1})$: The counterterm of any such subdiagram carries now a factor m^2, such that the counterterm of the remaining diagram, which is a pure factor of zero dimension, cannot depend on $\mathbf{k}^2$. Thus such counterterms will not appear in $Z_\phi(g,\varepsilon^{-1})$ obtained from Eq. (11.31) via a momentum differentiation. Diagrams with tadpole parts contribute only to the mass renormalization, but not to $Z_\phi(g,\varepsilon^{-1})$.

The remaining quadratically divergent diagrams without tadpole parts depend on the external momentum. Carrying out the differentiation with respect to this momentum,

$$\frac{\partial}{\partial\mathbf{k}^2}\mathcal{K}R\bar{\Gamma}^{(2)}(\mathbf{k},m^2) \;=\; \mathcal{K}\bar{R}\frac{\partial}{\partial\mathbf{k}^2}\bar{\Gamma}^{(2)}(\mathbf{k},m^2)\;, \tag{11.44}$$

generates logarithmically divergent integrals. The differentiation can always be interchanged with the R-operation [4]. In a Feynman integral some terms may depend on the individual components k_μ of $\mathbf{k}$ rather than on $\mathbf{k}^2$. When performing the differentiations in such terms, we use the relation

$$\frac{\partial}{\partial\mathbf{k}^2} = \frac{1}{2D}\frac{\partial^2}{\partial k_\mu\partial k_\mu}, \tag{11.45}$$

which follows from the trivial equation

$$\frac{\partial^2}{\partial k_\mu\partial k_\mu}\,\mathbf{k}^2 \;=\; 2\,D\;. \tag{11.46}$$

In $D \equiv 4 - \varepsilon$ dimensions, the differentiations are done as follows:

$$\frac{\partial}{\partial k_\mu} \frac{1}{(\mathbf{p}-\mathbf{k})^2 + m^2} = -\frac{2(p-k)_\mu}{[(\mathbf{p}-\mathbf{k})^2 + m^2]^2} \tag{11.47}$$

$$\frac{\partial^2}{\partial k_\mu \partial k_\mu} \frac{1}{(\mathbf{p}-\mathbf{k})^2 + m^2} = \frac{-2D}{[(\mathbf{p}-\mathbf{k})^2 + m^2]^2} + \frac{8\,(\mathbf{p}-\mathbf{k})^2}{[(\mathbf{p}-\mathbf{k})^2 + m^2]^3}. \tag{11.48}$$

The differentiation raises the power of the denominator by one unit and multiplies the numerator by the loop vector. Diagrammatically, this raising of power may be attributed to the presence of an additional $-\phi^2$-vertex. If we indicate the momentum vector in the numerator by a vertical dash, we can express the operations (11.47) and (11.48) diagrammatically as

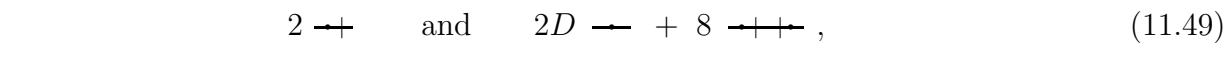

(11.49)

respectively. The line with the dash symbolizing the propagator $p_\mu/(\mathbf{p}^2 + m^2)$ and will be referred to as a *line with a vector index*.

Although these operations are quite lengthy, the result has at least the advantage of being less divergent. Moreover, they will lead to real simplifications due to the fact that the calculation of all counterterms can eventually be done with massless Feynman integrals. Then the propagators in the last expression can be combined to $(8 - 2D)/[(\mathbf{p} - \mathbf{k})^2]^2$. All such simplifications will be discussed in detail in Subsection 12.2.2.

Notes and References

Good textbooks explaining the R-operation are
N.N. Bogoliubov and D.V. Shirkov, *Introduction to the Theory of Quantized Fields*, Wiley Interscience, New York, 1958,
and
C. Itzykson and J.-B. Zuber, *Quantum Field Theory*, McGraw-Hill, New York, 1980.

The individual citations in the text refer to:

[1] See, in particular, Refs. [2] and [5] in Chapter 9.

[2] W. Zimmermann, Commun. Math. Phys. *16*, 208 (1969).

[3] J.C. Collins, Nucl. Phys. B **80**, 341 (1974);
E.R. Speer, J. Math. Phys. **15**, 1 (1974);
P. Breitenlohner and D. Maison, Commun. Math. Phys. **52**, 11, 39, 55 (1977);
W.E. Caswell and A.D. Kennedy, Phys. Rev. D **25**, 392 (1982).

[4] For a proof see
W.E. Caswell, A.D. Kennedy, Phys. Rev. D *25*, 392 (1982).